PCCP

Accepted Manuscript

ROYAL SOCIETY OF CHEMISTRY

www.rsc.org/pccp

Physical Chemistry Chemical Physics
CREATED USING THE RSC LaTeX PCCP ARTICLE TEMPLATE – SEE www.rsc.org/electronicfiles FOR DETAILS
ARTICLE TYPE www. rsc.org/xxxxxx | XXXXXXXX

Full cLR-PCM calculations of the solvatochromic effects on emission energies

Siwar Chibani[a], Šimon Budzák[b], Miroslav Medved'[b], Benedetta Mennucci*[c] and Denis Jacquemin*[a,d]

Received Xth XXXXXXXXXX 20XX, Accepted Xth XXXXXXXXX 20XX
First published on the web Xth XXXXXXXXXX 200X
DOI: 10.1039/b000000x

We compare the solvatochromic shifts measured experimentally and obtained theoretically for the emission of several fluorophores (indole, benzofurazan, naphthalimide...). Our theoretical protocol relies on Time-Dependent Density Functional Theory and uses several variations of the Polarisable Continuum Model. In particular, we compare the merits of the linear-response and the corrected linear response approaches, the latter being used for both energetic and structural calculations. It turns out that performing fully-consistent corrected linear response calculations yields the smallest mean signed and absolute errors for the solvatochromic shifts, although optimizing the excited-state structures at the linear-response level only induces limited increase of the average deviations. On the contrary, for auxochromic effects, the average errors provided by the two solvation models are very similar.

1 Introduction

The exploration of the potential energy surfaces of electronically excited-states (ES) with theoretical tools is a field of extremely active research, as direct experimental measurements of ES geometries are very difficult to achieve but for tiny molecules. In that framework, Time-Dependent Density Functional Theory (TD-DFT),[1,2] remains the most widely used first-principles approach and this can be explained by:[3,4] i) the moderate computational cost; ii) the implementation of first and second TD-DFT derivatives making both ES geometry optimisations and ES vibrational calculations straightforward;[5–7] iii) the relative ease to prepare and analyze TD-DFT calculations;[8,9] and iv) the development of a large panel of approaches allowing to account for environmental effects.[10,11] Indeed, several declinations of the Polarizable Continuum Model (PCM)[12] that provides an efficient assessment of the impact of solvents have been proposed to tackle ES during the last fifteen years. This includes the linear response (LR),[13,14] the corrected linear response (cLR),[15] the state specific (SS)[16] and the vertical excitation model (VEM)[17] PCM approaches. In the simpler LR approach,[13,14] the ground-to-excited transition densities are used to determine the variations of the charges localized on the PCM cavity when the solute goes from its ground-state (GS) electronic configuration to one of its electronically ES. In the perturbative cLR scheme, the one-particle TD-DFT density matrix, that accounts for the orbital relaxation contribution, is used to determine the variations of the charges of the cavity.[15] In the SS and VEM approximations, a self-consistent formulation is used with (SS)[16] or without (VEM)[17] modifying the ground-state reference. These three refined approaches provide a more physically sound description of the solvent response to the ES than the LR model, especially for emission energies. However, except for our very recent works (see below) the PCM-TD-DFT gradients are only available within the LR approach.[18] Consequently, a widely-applied protocol to determine fluorescence wavelengths of solvated dyes is to perform LR-PCM TD-DFT optimisation to obtain ES geometries, and, next, to compute single point vertical cLR/SS-PCM emission energies on these geometries. Of course, such hybrid approach is only accurate when the LR scheme correctly models the solvent effects on the ES geometries.

Very recently, we have performed the first cLR ES geometry optimisations of six model compounds, allowing to obtain full cLR emission energies[19] as well as cLR ES polarisabilities.[20] In Ref. 19, we showed that the LR method often exaggerates the solvent-induced geometrical changes compared to the gas-phase reference. For a small π-conjugated compound, namely thieno[2,3-*b*]thiophene, it was found that the cLR emission energies computed on the optimal LR and cLR

[a] *Chimie Et Interdisciplinarité, Synthèse, Analyse, Modélisation (CEISAM), UMR CNRS no. 6230, BP 92208, Université de Nantes, 2, Rue de la Houssinière, 44322 Nantes, Cedex 3, France. E-mail: denis.jacquemin@univ-nantes.fr.*
[b] *Department of Chemistry, Faculty of Natural Sciences, Matej Bel University, Tajovského 40, SK-97400 Banská Bystrica, Slovak Republic.*
[c] *Department of Chemistry, University of Pisa, Via Risorgimento 35, 56126 Pisa, Italy. E-mail: benedetta.mennucci@unipi.it.*
[d] *Institut Universitaire de France, 103, blvd Saint-Michel, F-75005 Paris Cedex 05, France.*

ES geometries differ by more than 0.2 eV, but the discrepancies were significantly smaller for the other five molecules. In another work,[21] we have investigated the solvation effects for dyes presenting an excited-state of cyanine nature, and showed that the total difference between LR and cLR emission energies can be mainly attributed to an electronic (rather than a geometric) effect for that specific chromogenic class. Despite these earlier works, it remains unclear if cLR ES structures provide an effectively improved accuracy compared to their LR counterparts. Indeed, in all these previous investigations, no comparisons with experimental values were made as the discussions were focussed on gas–LR–cLR differences for a given solvent. In addition, the size of the molecular sets was too small to allow statistically-significant conclusions. In the present contribution, we lift these limits by: i) investigating a large set of fluorophores (see Figure 1 and Table 1); ii) focussing our analysis on systems for which emission energies are available in several solvents or several substitution patterns have been used; iii) providing a statistical analysis for all possible blends of the gas, LR and cLR models. To the very best of our knowledge, this is the first work providing fluorescence solvatochromic shifts with a fully consistent cLR-PCM model. Let us note that we study the lowest $\pi \rightarrow \pi^{\star}$ ES of the compounds shown in Figure 1, several presenting a quite localized nature, though a significant intramolecular charge-transfer between the two cycles takes place in several indoles and benzofurazans.

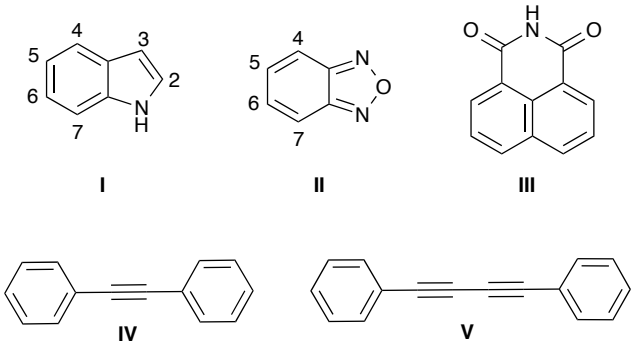

Fig. 1 Compounds investigated in the present study with numbering of the substitution positions for indoles (**I**) and benzofurazans (**II**).

2 Computational details

The used computational protocol follows the one discussed in our previous works,[19,21] and is only briefly summarised here. All calculations have been performed with the Gaussian09 program[32] but for the cLR optimisation of the ES geometries that were determined with a locally-modified version.[19] Improved energy (at least 10^{-10} a.u.) and geometry (10^{-5} a.u. on the residual root mean square force) convergence thresholds have been applied whereas a tighter DFT integration grid (so-called *ultrafine* grid) was used. Default parameters have been used for the PCM cavity and we have considered a large list of solvents, i.e., cyclohexane (CH), *n*-hexane (HEX), ethyl acetate (EA), diethylether (DEE), dichloromethane (DCM), acetonitrile (ACN), ethanol (EtOH) and water (WAT), so to fit available experimental data. To obtain excited-state geometries, we have first performed gas-phase and LR-PCM TD-DFT geometry optimisations using the analytical gradients implemented in Gaussian09.[33] Point group symmetry was used when possible to lighten the computational burden. Numerical Hessian calculations at the LR-PCM TD-DFT level have been achieved to ascertain the absence of imaginary frequencies. cLR-PCM TD-DFT optimisations were next carried out, using the procedure described in Ref. 19. Note that this procedure relies on forces obtained through numerical differentiation of the total cLR energies and is therefore much more computationally demanding than LR-PCM optimisations that use analytical gradients. All these structural calculations have been performed at the PBE0/6-31G(d) level.[34,35] The vertical emission energies have been determined through single-point TD-DFT calculations using the PBE0/6-311+G(2d,p) approach. Note that the specific choice of a particular exchange-correlation functional might tune the computed emission wavelengths, but we are mostly interested in both auxochromic and solvatochromic effects. Therefore, this functional dependence is strongly attenuated here. This is further discussed in the next Section. The solvent geometry optimisations have been performed in the equilibrium LR-PCM or cLR-PCM limit whereas the reported emission wavelengths have been computed in both the equilibrium (LR-PCM and cLR-PCM) and non-equilibrium (cLR-PCM) limits. In the present cases, the nonequilibrium scheme refers to an equilibrated excited state followed by a vertical nonequilibrium ground state calculation; as such a scheme is not applicable to a LR formulation only cLR(neq) data are reported. Of course, using the PCM approach also implies several approximations that may impact the results. This includes the lack of explicit interactions with solvent molecules close to the chromophores, as well as the neglect of non-electrostatic contributions to the transition energies.

In the following, we have chosen to list fluorescence data in the wavelength scale (nm, generally favored in experimental papers) but the statistical analysis has been performed in both nm and eV scales.

Table 1 Theoretical emission wavelengths (in nm) computed for the systems shown in Figure 1 using different combinations of PCM approaches and applying the TD-PBE0/6-311+G(2d,p)//PBE0/6-31G(d) approach. Experimental values are given at the right of the Table. eq and neq stand for equilibrium and non-equilibrium PCM limits, respectively.

			Gas-phase geometry				LR-PCM geometry				cLR-PCM geometry				
	Subst.	Solvent	Gas	LR (eq)	cLR (eq)	cLR (neq)	Gas	LR (eq)	cLR (eq)	cLR (neq)	Gas	LR (eq)	cLR (eq)	cLR (neq)	Exp.
I	–	CH	294.2	298.4	298.2	298.1	294.4	298.6	298.2	298.1	295.7	299.6	300.1	300.0	288[22] 298[23] 297[24]
		ACN	294.2	305.6	305.5	310.3	294.8	307.3	304.9	309.0	298.2	308.3	313.2	320.1	320[23]
	3-Me	CH	312.6	317.3	318.8	318.7	312.3	317.1	318.3	318.2	314.3	318.9	321.0	321.0	305[22] 315[24]
	5-Br	HEX	299.1	303.1	303.6	303.5	300.0	304.2	304.6	304.6	301.6	305.7	306.8	306.8	303[23]
		EA	299.1	308.4	310.0	313.5	300.3	310.4	311.4	314.9	303.4	312.7	317.6	322.4	314[23]
	5-Cl	CH	299.0	303.6	304.2	304.1	299.6	304.3	304.8	304.7	301.2	305.8	307.1	307.0	309[22]
	5-CN	CH	316.5	324.8	329.0	328.9	316.7	325.1	329.3	329.2	318.5	326.9	331.7	331.6	316[22]
		HEX[a]	316.5	324.0	327.8	327.8	317.0	324.8	328.5	328.4	318.3	326.0	330.2	330.2	316[23] 315[25]
		EA	316.5	333.3	344.2	351.0	316.9	334.2	350.0	351.8	320.4	338.0	351.6	359.6	345[23]
		ACN	316.5	338.3	354.3	365.9	317.0	339.7	355.6	367.2	321.4	344.6	365.8	380.2	356[23] 361[25]
	5-F	CH	294.6	298.9	298.8	298.7	295.6	300.2	299.9	299.9	297.3	301.7	302.3	302.2	296[22]
	5-OH	CH	299.0	301.4	299.2	299.2	299.6	302.1	299.9	299.9	298.9	301.3	299.1	299.1	322.5[22]
		EA	299.0	304.2	299.6	300.3	300.4	305.9	301.1	301.8	298.8	304.1	299.5	300.2	330[26]
		ACN	299.0	306.1	299.9	301.1	300.9	308.5	301.9	303.0	298.7	305.9	299.8	301.0	330[26]
	5-NH_2	CH	329.0	333.2	331.9	331.9	331.7	335.3	333.9	333.8	329.9	334.4	333.2	333.2	347[22] 352[27]
		DEE	329.0	336.6	334.3	336.2	331.6	340.3	337.7	339.5	330.1	338.3	336.2	338.2	362[27]
		ACN	329.0	340.6	337.2	340.9	332.2	345.7	341.5	345.2	329.9	342.4	339.5	343.5	368[27]
II	4-NH_2	CH	476.5	501.5	507.8	506.9	476.5	501.8	507.3	507.2	478.3	503.9	510.4	510.2	483.5[22]
	4-SMe	CH	436.4	456.7	459.5	459.4	437.4	458.1	460.6	460.4	437.8	457.1	461.1	461.0	433.5[22]
	5-NH_2	CH	409.6	426.0	426.8	426.7	410.6	427.2	428.0	428.0	410.0	426.6	428.0	428.0	424[22] 423[28]
		DCM	409.6	447.9	453.4	462.6	412.0	451.6	456.8	466.0	410.3	449.9	459.1	469.7	462[28]
		ACN	409.6	454.8	462.6	476.6	412.5	459.4	466.9	480.9	410.3	457.2	470.8	487.3	487[28]
	5-OMe	CH	364.2	374.7	373.8	383.8	365.3	376.0	375.1	375.1	364.9	375.6	375.0	375.0	350[22] 372[28]
		DCM	364.2	388.8	388.3	392.8	366.6	392.0	391.7	396.4	365.3	390.9	392.8	398.1	394[28]
		ACN	364.2	393.2	393.2	399.9	366.9	397.1	397.3	404.4	365.4	395.7	399.2	407.4	403[28]
III		HEX	351.6	358.3	352.4	352.4	365.2	372.6	366.3	366.2	351.6	358.3	352.5	352.4	376[29]
		EtOH	351.6	372.6	354.7	355.1	366.4	389.5	369.8	370.2	364.0	386.8	367.5	368.1	370[30] 384[29]
IV		EtOH	336.1	367.5	334.0	334.4	341.4	374.8	339.3	339.7	336.7	368.2	334.6	335.0	302[31]
V		EtOH	394.3	424.6	391.0	391.3	398.3	430.5	394.9	395.3	395.2	425.7	391.9	392.3	326[31]

[a] *n*-hexane or isopentane depending on the experimental reference.

3 Results

3.1 Basis set and functional effects

To evaluate the convergence of our results with respect to the size of the atomic basis set, we have selected 5-CN-**I** as example (in cyclohexane). If one uses the extremely extended 6-311++G(3df,3pd) atomic basis set instead of its 6-311+G(2d,p) counterpart for the calculation of vertical emission energies, we notice no variations of the absolute transition wavelengths larger than 0.4 nm irrespective of the selected geometry of solvation model, the relative differences when shifting from one solvation model to another being even smaller. We also optimized the excited-state geometries using 6-311++G(d,p) instead of 6-31G(d). Considering the 6-311++G(d,p) [6-31G(d)] optimal gas phase structure, we obtain 315.1 [316.5], 323.0 [324.8], 327.0 [329.0] and 326.9 [328.9] nm for gas, LR(eq), cLR(eq) and cLR(neq) 6-311+G(2d,p) emission wavelengths, respectively. This means that the solvatochromic shifts are almost unaffected by selected basis set, e.g., the cLR(neq)–gas variation is -11.8 [-12.4] nm considering the 6-311++G(d,p) [6-31G(d)] structure, hinting that our selection of atomic basis sets was suitable for our purposes.

For the same compound, we have also evaluated the data obtained when three popular hybrid functionals, namely B3LYP,[36] M06-2X[37] and CAM-B3LYP[38] to determine the emission transition energies, and compared them to PBE0 results.[39] As expected, we found that the absolute transition energies tend increase with the amount of exact exchange included in the exchange-correlation functional. For instance, the LR(eq)//gas[40] emission wavelengths are 334.3, 324.8, 303.4 and 300.7 nm with B3LYP, PBE0, CAM-B3LYP and M06-2X respectively. While these changes are significant (more than 30 nm between CAM-B3LYP and B3LYP) and well-documented,[41] the impact of the selected functional on the solvatochromic shifts is much smaller. This can be illus-

trated, on the one hand, by investigating the cLR(neq)//gas–gas//gas shifts that attain +13.3, +12.4, +9.4 and +9.5 nm, for the same four approaches, and, on the other hand by computing cLR(neq)//cLR(neq)–cLR(neq)//gas shifts that attain +3.0, +2.7, +1.4 and +1.5 nm, for these found functionals, respectively.[39] Therefore both the direct (electronic) and indirect (geometric) solvation effects are much less affected by the choice of a specific exchange-correlation functional than the absolute transition energies, though we notice that functionals including larger ratio of exact exchange tend to lead to smaller solvatochromic shifts.

3.2 Solvatochromism

Table 1 collects the computed data for all treated systems using all possible combination of gas, LR and cLR approximations for determining both the ES geometries and the emission energies. As it can be seen in the leftmost column, the experimental emission wavelengths reported in the literature might vary significantly from one reference to another, e.g. 10 nm for 3-Me-**I** in cyclohexane, 22 nm for 5-OMe-**II** in cyclohexane and 14 nm for **III** in ethanol. Therefore, depending on the selected reference values, one could conclude that the emission band of **III** undergoes positive or negative solvatochromism when going from *n*-hexane to ethanol. Some of these differences could probably be ascribed to slightly different experimental protocols (e.g., different temperature). Therefore, we have chosen to consider only solvatochromic effects reported in a given work, rather than calculate effects from data collected in two different publications. This leaves a set of 12 linearly-independent solvatochromic shifts. For 5-CN-**I**, two results can be computed when going from *n*-hexane to acetonitrile: 40 nm[23] and 46 nm.[25] We have used the average value in that case.

Table 2 provides a statistical analysis of solvatochromic shifts in terms of mean signed and mean absolute errors (MSE and MAE, respectively). The standard deviation (SD) is provided as well. The gas//gas approach obviously yields 100% error as no solvatochromic shift can be estimated, and the reported data are therefore a measure of the average solvatochromic shift present in the set, that is, 24.6 nm. Performing LR(eq)//gas calculations gives a MAE of 13.8 nm. In other words, this method only provides ca. 50% of the experimental solvatochromic effects, a large error that can be decreased with the cLR(neq)//gas method (MAE of 7.1 nm). By investigating the impact of the environmental model used during the geometry optimisation, one notices nearly systematic improvements when using LR and next cLR. In particular the cLR(neq)//cLR(eq) method, the *a priori* more refined and sound scheme, provide a trifling MSE ($<$ 1 nm) and the smallest MAE of the series (3.6 nm) though the improvements with respect to the standard cLR(neq)//LR(eq) model remain negligible for this latter parameter. The SD obtained with cLR(neq)//cLR(eq) is 4.5 nm slightly larger than the one obtained with cLR(neq)//LR(eq) (3.9 nm), but the reverse holds on the eV scale. With cLR(neq)//cLR(eq), the two largest theory-experiment discrepancies are obtained, on the one hand, for **III** (7.7 nm error) but a protic solvent, not ideal for PCM calculations is involved in that specific case (*n*-hexane to ethanol), and, on the other hand, for 5-CN-**I** (7.0 nm error when going from *n*-hexane to acetonitrile), but the relative error remains limited (ca. 16%: 43.0 nm experimentally *versus* 50.0 nm theoretically).

In Figure 2 we provides the comparison between experiment and theory for the cLR(neq)//cLR approach and the obtained MSE and MAE are limited to 3.8 nm (-0.026 eV) and 16.3 nm (0.166 eV), respectively. These errors are well within the expected accuracy of TD-DFT.[41] Of course, as stated above, absolute deviations are not a relevant measure of the quality of the environmental model, as the selected exchange-correlation functional plays a significant role in the final accuracy. We have therefore moved our attention on the obtained linear determination coefficient, R^2. Irrespective of the selection of the LR or cLR geometries we obtained R^2 of 0.77, 0.78, 0.87 and 0.88 for gas, LR(eq), cLR(eq) and cLR(neq) fluorescence wavelengths, respectively. Clearly, cLR provides more consistent results than LR, but this effect has a sole electronic origin.

In summary, we have demonstrated, for the first time, that full cLR calculations provide very accurate solvation shifts for emission energies, and that the cLR structural corrections, though quite small, statistically improve the LR results, no-

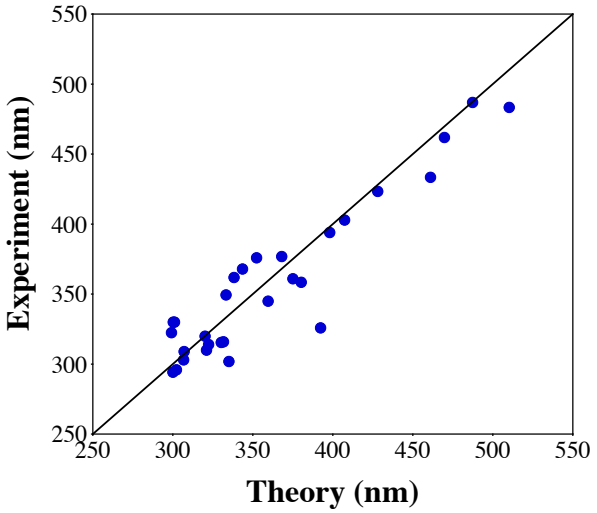

Fig. 2 Comparison between cLR(neq)//clR and experimental emission wavelengths for the full set of compounds listed in Table 1. The central line indicates a perfect theory-experiment match.

Table 2 Mean signed error, mean absolue error and standard deviation obtained for the twelve linearly independent solvatochromic shifts.

		Gas-phase geometry				LR-PCM geometry				cLR-PCM geometry			
		Gas	LR (eq)	cLR (eq)	cLR (neq)	Gas	LR (eq)	cLR (eq)	cLR (neq)	Gas	LR (eq)	cLR (eq)	cLR (neq)
nm	MSE	-24.6	-12.4	-11.0	-7.0	-23.8	-10.6	-9.2	-4.0	-22.6	-9.8	-6.1	0.7
	MAE	24.6	13.8	11.0	7.1	23.9	12.5	9.4	4.2	23.4	13.5	7.4	3.6
	SD	17.9	11.8	7.2	5.0	17.6	11.8	6.8	3.9	19.0	13.4	6.8	4.5
eV	MSE	0.219	0.109	0.099	0.064	0.212	0.095	0.084	0.040	0.197	0.086	0.055	-0.002
	MAE	0.219	0.124	0.099	0.066	0.213	0.113	0.086	0.043	0.206	0.121	0.068	0.030
	SD	0.137	0.106	0.060	0.043	0.138	0.108	0.061	0.042	0.144	0.117	0.058	0.038

tably by decreasing the MSE.

3.3 Structural and geometrical effects

We complete the previous analysis by dissecting the structural and geometrical effects.

To start, we consider auxochromic shifts (in a given solvent) to ascertain which environmental model provides the most consistent estimates. Again, we have followed the previously-defined strategy of selecting only data originating from a single publication. In the present case, we have kept the solvent constant and investigated the impact of the variations of the substituents. This leads to a set of 14 independent auxochromic shifts for indoles and benzofurazans for which a statistical analysis is given in Table 3. The average auxochromic effect for the selected compounds is 45.9 nm or -0.412 eV. Considering a given geometry, one notices that including solvent effects in the calculation of transition energies only slightly decrease the MAE, but significantly improves the MSE. On the contrary, the SD unexpectedly tend to be deteriorated when solvent effects are considered, especially with the cLR scheme. By comparing the cLR(neq)//cLR and cLR(neq)//LR results, one notices almost unchanged MAE (variations 0.5 nm or 0.001 eV), MSE (changes of +0.9 nm or +0.003 eV) and SD (differences of -1.3 nm or -0.007 eV). In other words, performing cLR optimization of the ES structures does not significantly improve, nor worsen, the computed auxochromic shifts.

As a further effect due to structural modifications of the solute, we can also consider the increase of the conjugation length: when going from **IV** to **V**, the experimental fluorescence wavelength is redshifted by 24 nm. Indepedently of the selected solvent approach, theory strongly overestimates this effect, as the TD-DFT shifts are in the 55–58 nm range. We attribute this error to the linear-response TD-DFT approximation and/or to the limits of the selected exchange-correlation functional.

Finally, we have analyzed the purely geometrical effect by comparing the cLR(neq) results obtained on the gas, LR and cLR geometries.

In general geometrical differences between cLR and LR are small and we could find no systematic trends, e.g., the cLR geometry does not always provide larger or smaller transition wavelengths than its LR counterpart, nor are the cLR values systematically bracketed by the wavelengths obtained on the corresponding gas and LR structures. We found only three cases in which the cLR(neq) absolute wavelengths (Δ^{geom}) obtained with cLR and LR geometries differ by more than 10 nm: i) unsubstituted indole in acetonitrile, for which Δ^{geom} attains +11.1 nm; ii) 5-CN-**I** in acetontrile (Δ^{geom}=+13.0 nm) for which the cLR optimization induces a significant redshift of +14.3 nm that can be compared to the much smaller +1.3 nm obtained with LR; and iii) naphthalimide, **III**, in *n*-hexane, for which the LR (cLR) optimization yields a +13.8 (0.0) nm variation of the gas-phase reference, yielding a Δ^{geom} of -13.8 nm. For the indoles, one notes that for the 5-OH and 5-NH_2 derivatives the Δ^{geom} are much smaller. To understand this phenomena, we have determined the charge-transfer parameters following Le Bahers' approach.[42]. The charge transfer distance (in ACN) are 0.67, 1.59, 1.80 and 2.49 Å for 5-OH-**I**, 5-NH_2-**I**, **I** and 5-CN-**I**, respectively. More striking are the excited-state dipole moments that respectively reach 2.31, 3.23, 7.18 and 17.44 D for the same four compounds. Clearly, more polar molecules in the ES yield larger Δ^{geom}, at least in a homologous series of chromogens.

4 Conclusions

We have investigated the emission wavelength of a large set of fluorophores in various media (32 cases) by combining Time-Dependent Density Functional Theory (PBE0) to several flavours of the Polarizable Continuum Model. In particular, this work focussed on the impact of optimizing the excited-state geometries going beyond the common LR formulation by introducing the corrected linear-response approach. It turned out that: i) the smallest signed and absolute errors for the solvatochromic shifts are obtained when using cLR for both structural and energetic calculations, though the impact of cLR optimisation is statistically limited; ii) for auxochromic shifts including solvation effects decreases the

Table 3 Mean signed error, mean absolue error and standard deviation obtained for the fourteen linearly independent auxochromic shifts obtained for **I** and **II**.

		Gas-phase geometry				LR-PCM geometry				cLR-PCM geometry			
		Gas	LR (eq)	cLR (eq)	cLR (neq)	Gas	LR (eq)	cLR (eq)	cLR (neq)	Gas	LR (eq)	cLR (eq)	cLR (neq)
nm	MSE	-13.6	-7.7	-3.2	-2.5	-13.6	-7.7	-2.8	-1.6	-13.4	-6.9	-2.4	-0.7
	MAE	15.4	11.4	11.1	12.0	15.2	11.1	11.3	11.1	15.4	10.8	11.3	11.6
	SD	13.1	12.7	15.0	15.5	12.8	12.1	14.6	15.0	13.6	13.3	15.7	16.3
eV	MSE	0.119	0.093	0.057	0.055	0.119	0.094	0.053	0.047	0.120	0.090	0.058	0.050
	MAE	0.138	0.119	0.126	0.136	0.135	0.118	0.128	0.127	0.139	0.120	0.125	0.128
	SD	0.126	0.141	0.171	0.181	0.120	0.135	0.169	0.174	0.131	0.146	0.176	0.181

signed and absolute deviations, but the differences between LR and cLR approaches are insignificant; iii) the improvement brought by cLR for the overall theory-experiment match is significant but this can be attributed to the electronic part of the calculation; and iv) no systematic trends could be found when shifting from LR to cLR excited-state structures. Given the results obtained here, we clearly advocate the use of cLR rather than LR to determine the transition energies corresponding to emission especially if solvatochromism is investigated, while cLR optimisations, that imply a significant computational burden, are only worth the effort when one suspects the LR geometries to be inaccurate, e.g., when large differences between LR and gas-phase structures are found.

Acknowledgment

S.C thanks the European Research Council (ERC, Marches - 278845) for her PhD grant. S.B., M.M. and D.J. are grateful to the project *Mobilities - enhancing research, science and education at the Matej Bel University* (ITMS code: 26110230082, under the Operational Program Education financed by the European Social Fund). D.J. acknowledges the European Research Council (ERC) and the *Région des Pays de la Loire* for financial support in the framework of a Starting Grant (Marches - 278845) and a *recrutement sur poste stratégique*, respectively. B.M. thanks the ERC for financial support in the framework of the Starting Grant (EnLight - 277755). This research used resources of 1) the GENCI-CINES/IDRIS (Grant c2014085117), 2) CCIPL (*Centre de Calcul Intensif des Pays de Loire*) and 3) a local Troy cluster.

References

1 E. Runge and E. K. U. Gross, *Phys. Rev. Lett.*, 1984, **52**, 997–1000.
2 M. E. Casida, in *Time-Dependent Density-Functional Response Theory for Molecules*, ed. D. P. Chong, World Scientific, Singapore, 1995, vol. 1, pp. 155–192.
3 L. González, D. Escudero and L. Serrano-Andrès, *ChemPhysChem*, 2012, **13**, 28–51.
4 A. D. Laurent, C. Adamo and D. Jacquemin, *Phys. Chem. Chem. Phys.*, 2014, **16**, 14334–14356.
5 C. van Caillie and R. D. Amos, *Chem. Phys. Lett.*, 1999, **308**, 249—255.
6 F. Furche and R. Ahlrichs, *J. Chem. Phys.*, 2002, **117**, 7433–7447.
7 J. Liu and W. Z. Liang, *J. Chem. Phys.*, 2011, **135**, 184111.
8 A. Dreuw and M. Head-Gordon, *Chem. Rev.*, 2005, **105**, 4009–4037.
9 C. Adamo and D. Jacquemin, *Chem. Soc. Rev.*, 2013, **42**, 845–856.
10 D. Jacquemin, B. Mennucci and C. Adamo, *Phys. Chem. Chem. Phys.*, 2011, **13**, 16987–16998.
11 I. Corral, L. González and B. Mennucci, *Comput. Theor. Chem.*, 2014, **1040–1041**, v.
12 J. Tomasi, B. Mennucci and R. Cammi, *Chem. Rev.*, 2005, **105**, 2999–3094.
13 R. Cammi and B. Mennucci, *J. Chem. Phys.*, 1999, **110**, 9877–9886.
14 M. Cossi and V. Barone, *J. Chem. Phys.*, 2001, **115**, 4708–4717.
15 M. Caricato, B. Mennucci, J. Tomasi, F. Ingrosso, R. Cammi, S. Corni and G. Scalmani, *J. Chem. Phys.*, 2006, **124**, 124520.
16 R. Improta, G. Scalmani, M. J. Frisch and V. Barone, *J. Chem. Phys.*, 2007, **127**, 074504.
17 A. V. Marenich, C. J. Cramer, D. G. Truhlar, C. G. Guido, B. Mennucci, G. Scalmani and M. J. Frisch, *Chem. Sci.*, 2011, **2**, 2143–2161.
18 G. Scalmani, M. J. Frisch, B. Mennucci, J. Tomasi, R. Cammi and V. Barone, *J. Chem. Phys.*, 2006, **124**, 094107.
19 S. Chibani, A. D. Laurent, A. Blondel, B. Mennucci and D. Jacquemin, *J. Chem. Theory Comput.*, 2014, **10**, 1848–1851.
20 S. Budzak, M. Medved, B. Mennucci and D. Jacquemin, *J. Phys. Chem. A*, 2014, **118**, 5652–5656.
21 D. Jacquemin, S. Chibani, B. Le Guennic and B. Mennucci, *J. Phys. Chem. A*, 2014, **118**, 5343–5348.
22 T. Tsuji, M. Onoda, Y. Otani, T. Ohwada, T. Nakajima and K. Hirao, *Chem. Phys. Lett.*, 2009, **473**, 196–200.
23 M. Sun, *Ph.D. thesis*, Texas Tech University, 1974.
24 B. L. van Duuren, *J. Org. Chem.*, 1961, **26**, 2954–2960.
25 P. Jennings, A. C. Jones and A. R. Mount, *J. Chem. Soc., Faraday Trans.*, 1998, **94**, 3619–3624.
26 B. Sengupta, J. Guharay and P. K. Sengupta, *SpectroChim. Acta A*, 2000, **56**, 1213–1221.
27 H. K. Sinha, S. K. Dogra and M. Krishnamurthy, *Bull. Chem. Soc. Jpn.*, 1987, **60**, 4401–4407.
28 S. Uchiyama, K. Takehira, S. Kohtani, T. Santa, R. Nakagaki, S. Tobita and K. Imai, *Phys. Chem. Chem. Phys.*, 2002, **4**, 4514–4522.
29 V. Wintgens, P. Valat, J. Kossanyi, L. Biczok, A. Demeter and T. Berces, *J. Chem. Soc. Faraday Trans.*, 1994, **90**, 411–421.
30 M. S. Alexiou, V. Tychopoulos, S. Ghorbanian, J. H. P. Tyman, R. G. Brown and P. I. Brittain, *J. Chem. Soc. Perkin Trans. 2*, 1990, 837–842.
31 H. Du, R. A. Fuh, J. Li, A. Corkan and J. S. Lindsey, *Photochem. Photobiol.*, 1998, **68**, 141–142.
32 M. J. Frisch, G. W. Trucks, H. B. Schlegel, G. E. Scuseria, M. A. Robb,

J. R. Cheeseman, G. Scalmani, V. Barone, B. Mennucci, G. A. Petersson, H. Nakatsuji, M. Caricato, X. Li, H. P. Hratchian, A. F. Izmaylov, J. Bloino, G. Zheng, J. L. Sonnenberg, M. Hada, M. Ehara, K. Toyota, R. Fukuda, J. Hasegawa, M. Ishida, T. Nakajima, Y. Honda, O. Kitao, H. Nakai, T. Vreven, J. A. Montgomery, Jr., J. E. Peralta, F. Ogliaro, M. Bearpark, J. J. Heyd, E. Brothers, K. N. Kudin, V. N. Staroverov, R. Kobayashi, J. Normand, K. Raghavachari, A. Rendell, J. C. Burant, S. S. Iyengar, J. Tomasi, M. Cossi, N. Rega, J. M. Millam, M. Klene, J. E. Knox, J. B. Cross, V. Bakken, C. Adamo, J. Jaramillo, R. Gomperts, R. E. Stratmann, O. Yazyev, A. J. Austin, R. Cammi, C. Pomelli, J. W. Ochterski, R. L. Martin, K. Morokuma, V. G. Zakrzewski, G. A. Voth, P. Salvador, J. J. Dannenberg, S. Dapprich, A. D. Daniels, O. Farkas, J. B. Foresman, J. V. Ortiz, J. Cioslowski and D. J. Fox, *Gaussian 09 Revision D.01*, 2009, Gaussian Inc. Wallingford CT.

33 Note that for the 5-Br-**I**, the LR-PCM-TD-PBE0 frequency calculations returns a weak imaginary frequency for the planar (C_s) structure. As i) the gas phase calculations yield a proper C_s minimum; ii) LR-PCM-TD-DFT geometry optimisations starting with a twisted (C_1) structure failed to converged (spurious excited-states), we have sticked to the C_s structure for that compound.

34 C. Adamo and V. Barone, *J. Chem. Phys.*, 1999, **110**, 6158–6170.

35 M. Ernzerhof and G. E. Scuseria, *J. Chem. Phys.*, 1999, **110**, 5029–5036.

36 A. D. Becke, *J. Chem. Phys.*, 1993, **98**, 5648–5652.

37 Y. Zhao and D. G. Truhlar, *Theor. Chem. Acc.*, 2008, **120**, 215–241.

38 T. Yanai, D. P. Tew and N. C. Handy, *Chem. Phys. Lett.*, 2004, **393**, 51–56.

39 Those calculations have been performed with the 6-311+G(2d,p) atomic basis set, considering PBE0/6-31G(d) geometries and varying the functional used to determine the vertical emission energies.

40 We use the usual transition energies//geometry notation throughout.

41 A. D. Laurent and D. Jacquemin, *Int. J. Quantum Chem.*, 2013, **113**, 2019–2039.

42 T. Le Bahers, C. Adamo and I. Ciofini, *J. Chem. Theory Comput.*, 2011, **7**, 2498–2506.

Graphical Abstract

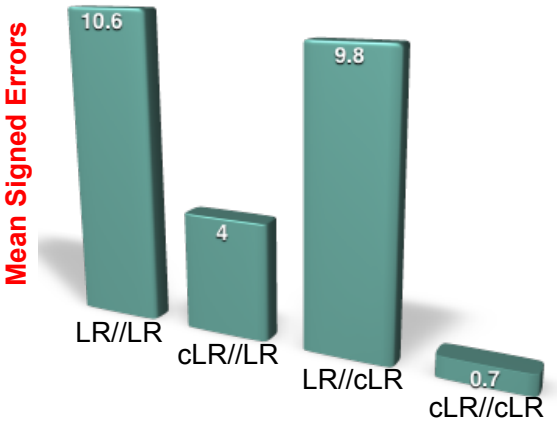

Are cLR-PCM excited-state geometries providing more accurate solvatochromic shifts ?